Supplementary Material S1 (SM1)

Morphology of minerals from Zn-rich chimneys of the Irinovskoe hydrothermal field, BSE images

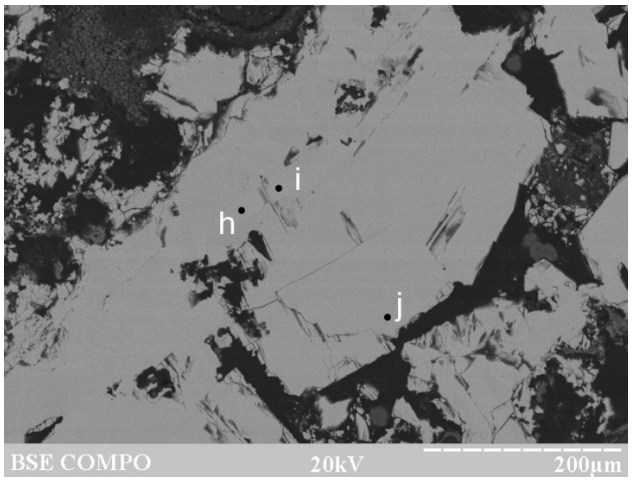

Figure S1-1. High-Fe low-Cd ZnS crystals (most likely, wurtzite) (h, j, i); sample 241-2/3-2, Image (hereinafter I) #35547.

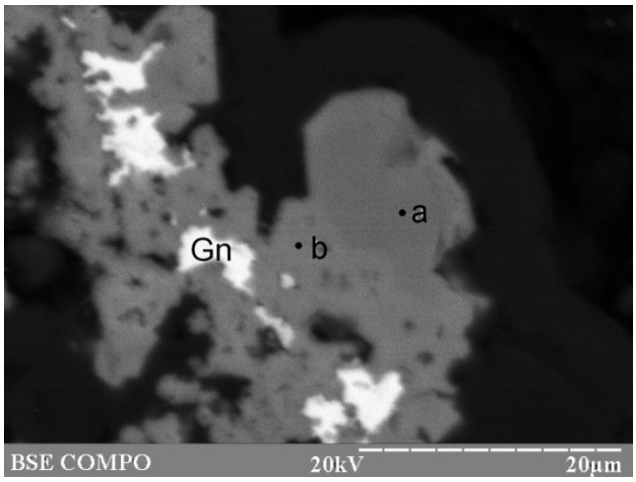

Figure S1-2. Interstitial galena (Gn) in crystalline Cd-poor Zn sulfide (a) replaced by Cd-rich Zn sulfide (b) from the rims; sample 241-2/1-11, I #34917.

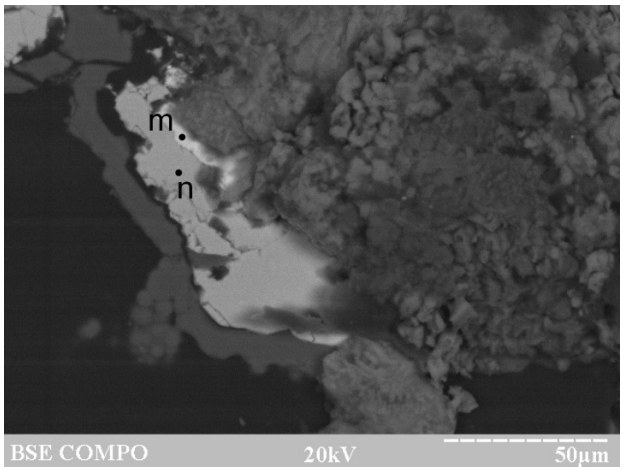

Figure S1-3. Rims of opal and Zn-bearing CdS phase (m) around Cd-free Zn sulfide (n); sample 241, I #35721.

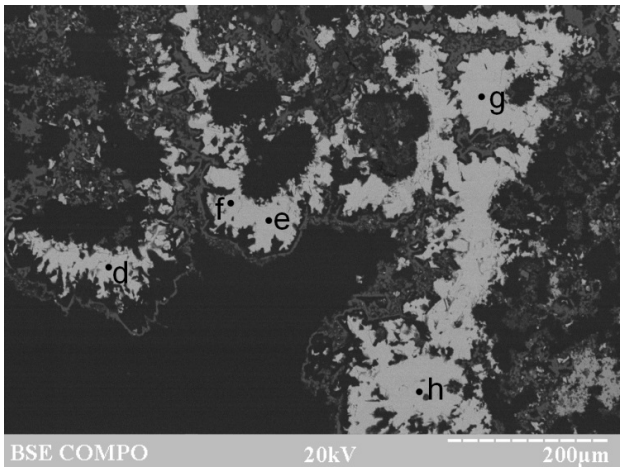

Figure S1-4. High-Fe low-Cd crystalline sphalerite (d, e, g, h) intergrown with chalcopyrite (f); sample 241-2/1-11, I #34922.

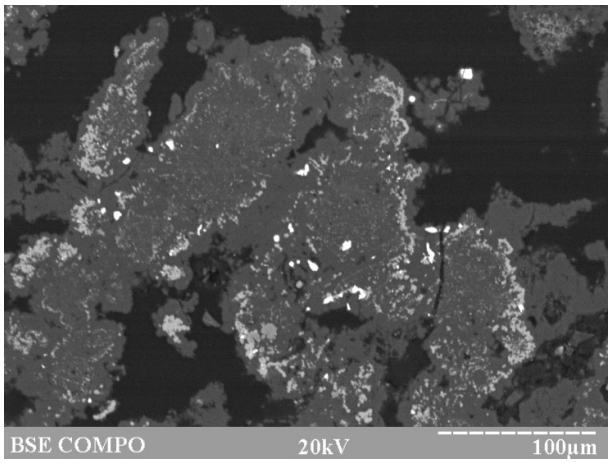

Figure S1-5. Zoned dendritic galena–sphalerite–opal aggregates; sample 241-2/1-11, I #34923.

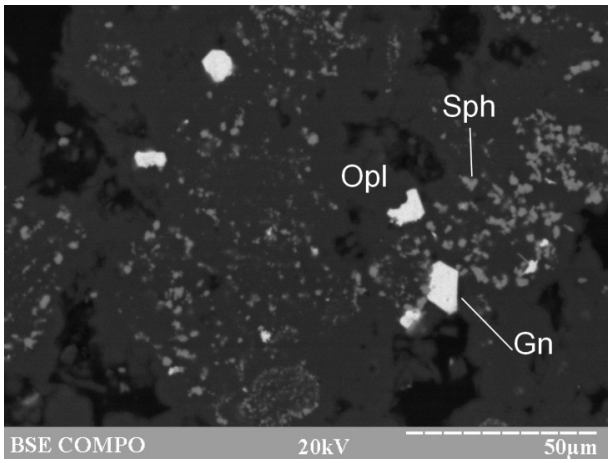

Figure S1-6. Inclusions of galena crystals and sphalerite grains (Sph) in opal (Opl); sample 241-2/1-11, I #34928.

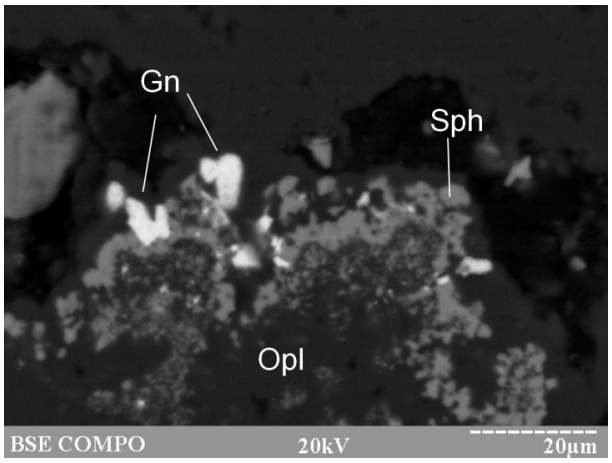

Figure S1-7. Opal rimmed by sphalerite with galena crystals on top; sample 241-2/1-11, I #34924.

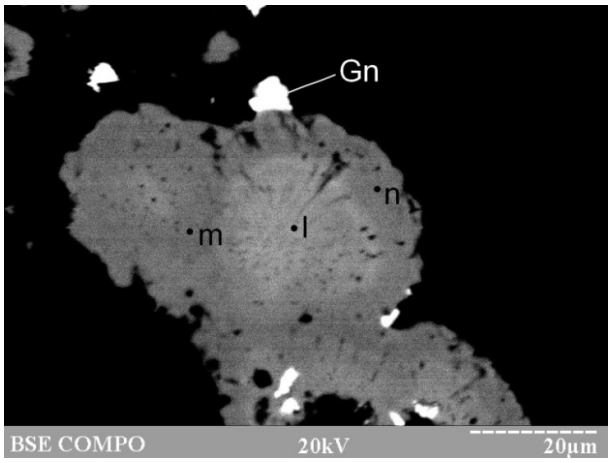

Figure S1-8. Zoned reniform aggregate of Fe-, Ag-, Pb-, and Cd-bearing Zn sulfide (l, m, n) with galena crystals on top; sample 241-2/1-11, I #34926.

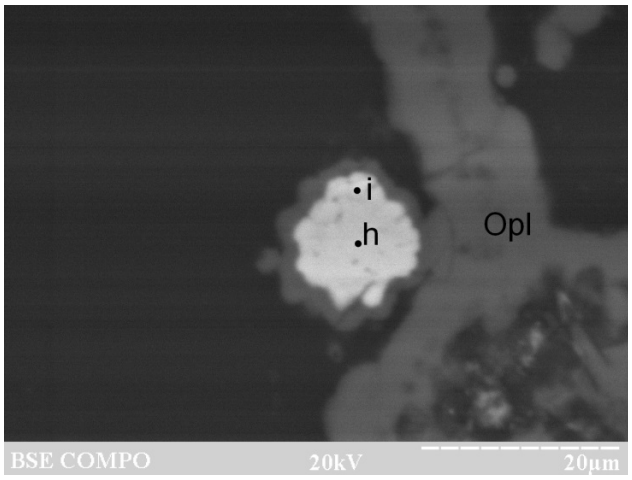

Figure S1-9. Pb-bearing (h) and Pb-free (i) framboidal sphalerite; sample 241-2/2-2, I #35658.

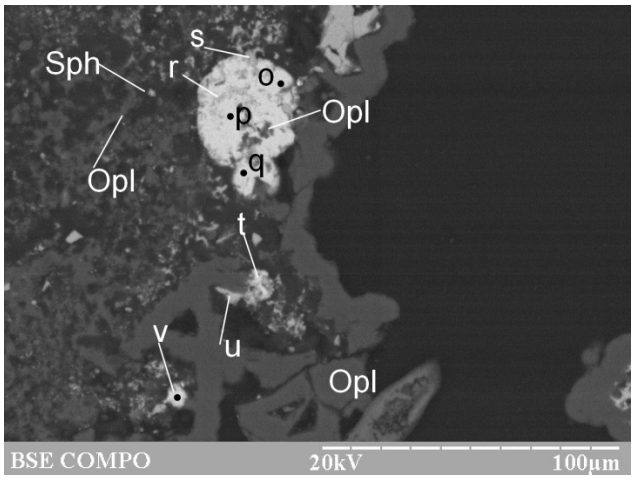

Figure S1-10. Replacement of reniform Cd-bearing sphalerite (r, s, u) by Zn-bearing CdS phase (o, p, q, t, v); sample 241, I #35722.

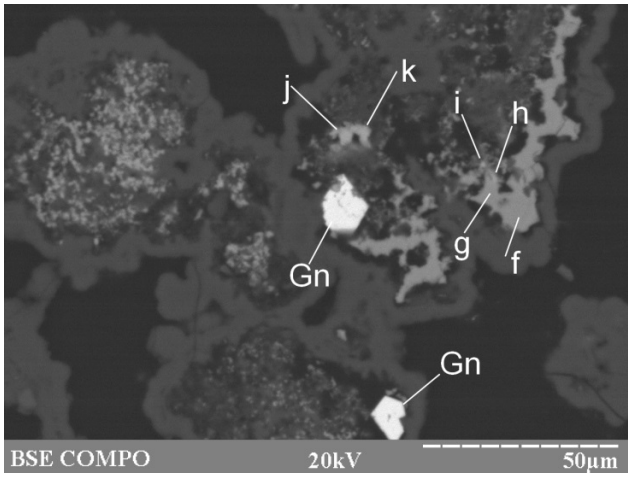

Figure S1-11. Galena and sphalerite (f, j) surrounded by a CdS–ZnS phase (h, i, j, k); sample 241-2/2-2, I #35620.

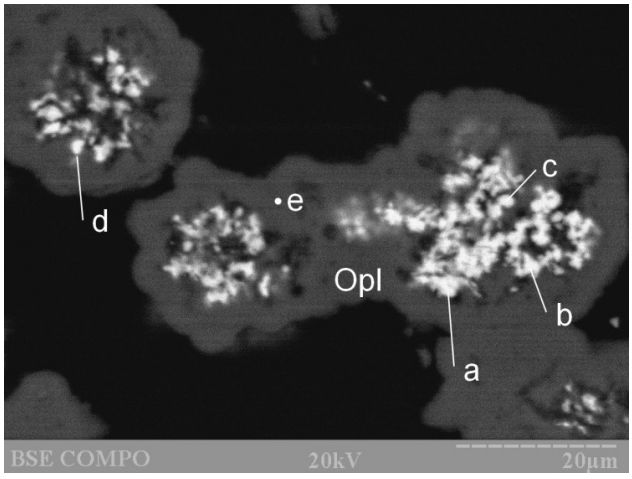

Figure S1-12. High-Cd sphalerite (a, b, c, d) in opal (e); sample 241-2/2-2, I #35619.

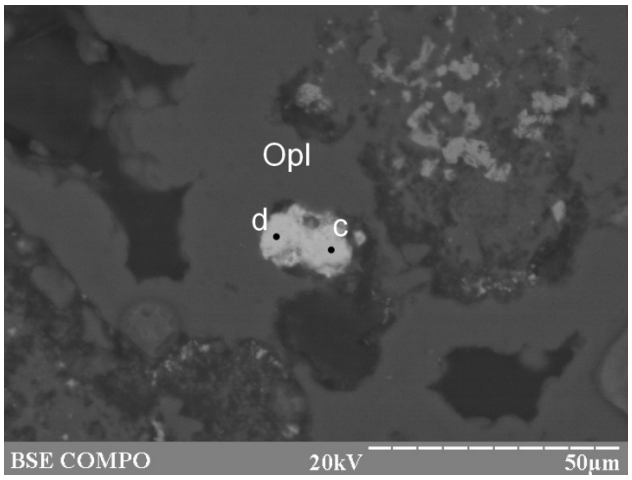

Figure S1-13. Aggregate of CdS phase (c, d) in opal; sample 241, I #35715.

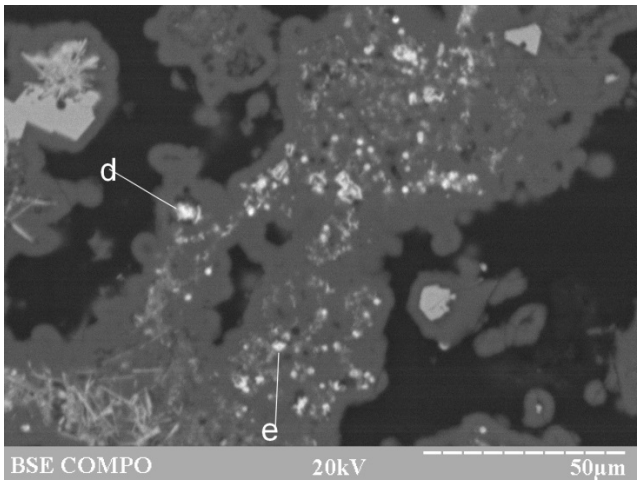

Figure S1-14. Inclusions of CdS phase (d, e) in opal; sample 241-2/2-2, I #35626.

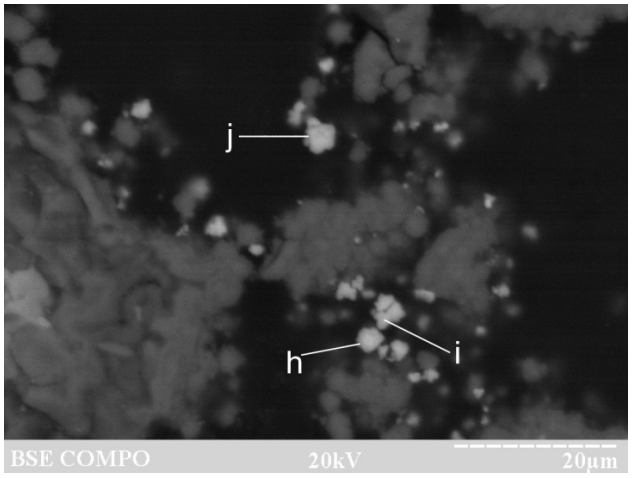

Figure S1-15. CdS phase (all points) on top of opal aggregates; sample 241-2/2-5, I #35002.

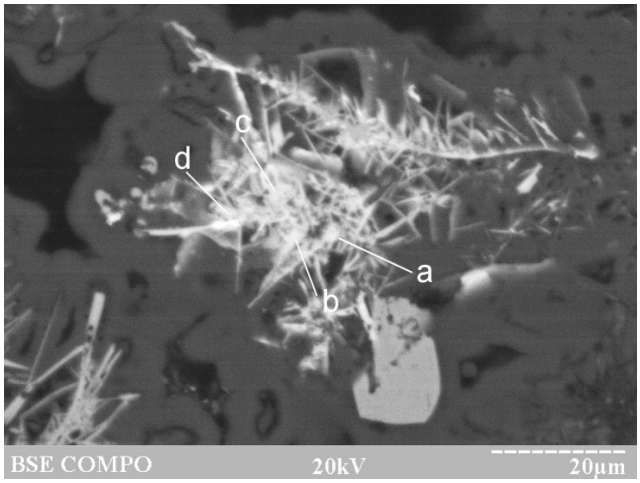

Figure S1-16. Latticework structure of acicular CdS phase (a, b, c, d); sample 241-2/2-2, I #35654.

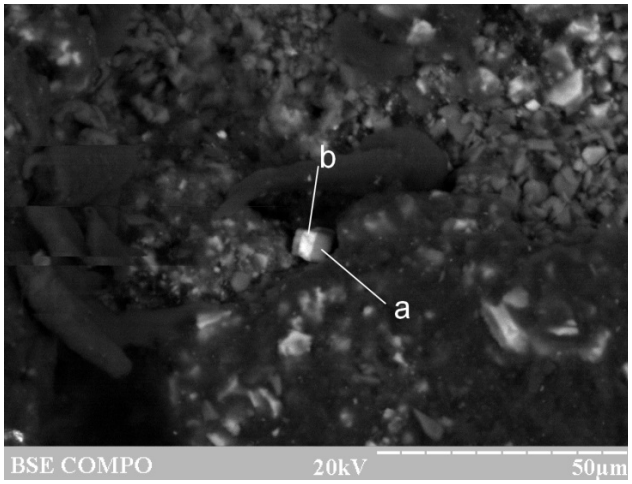

Figure S1-17. Platy lollingite grains (a) around platy As-bearing galena crystal (b); sample 241-2/2-4, I #35754.

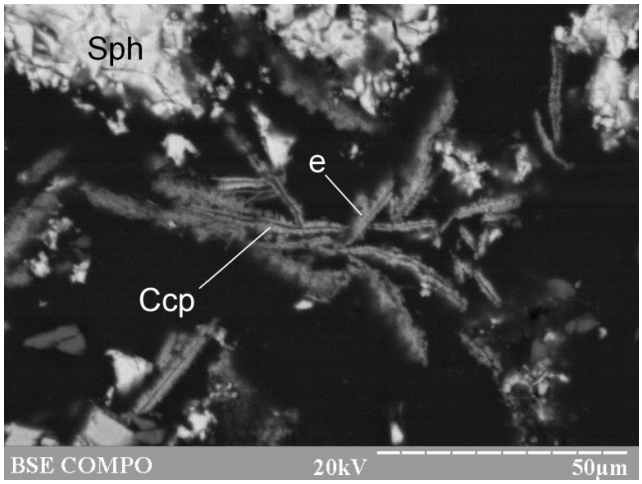

Figure S1-18. Filamentous chalcopyrite (Ccp) between sphalerite in opal (e); sample 241-2/3-2, I #35618.

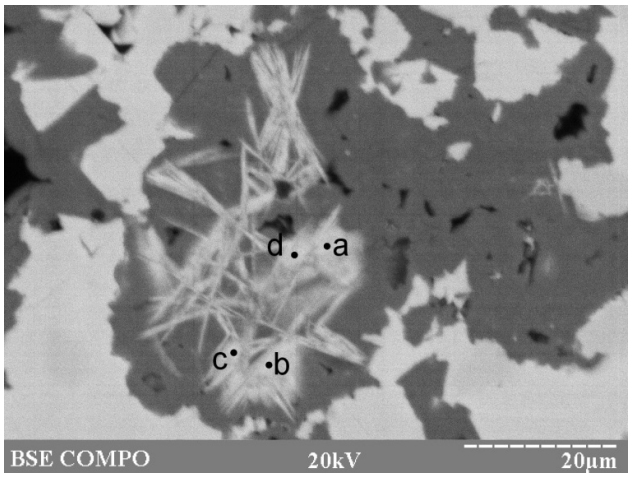

Figure S1-19. Radial aggregates of acicular covellite crystals (a–d) (Figure 7b) in Fe-oxyhydroxides, which replace Zn sulfide; sample 241-2/2-5, I #36257.

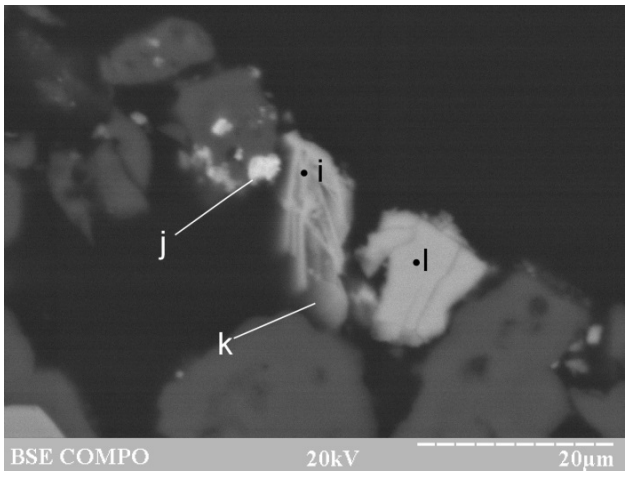

Figure S1-20. Low-Fe and low-Zn (i) and high-Fe and high-Zn (j, k) covellite and sphalerite (l); sample 241-2/2-2, I #35652.

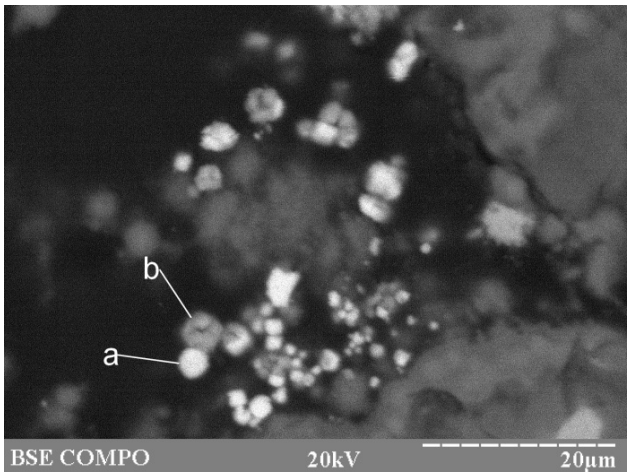

Figure S1-21. Assemblage of rounded grains of Ag-bearing covellite (b) and acanthite (a); sample 241-2/2-5, I #34999.

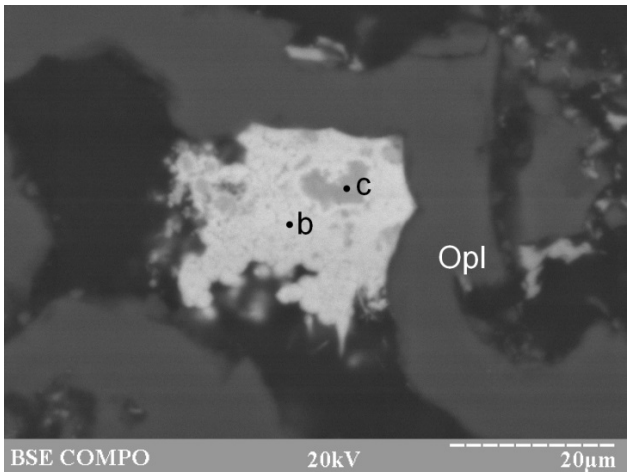

Figure S1-22. Replacement of Ag–Sb-bearing covellite (c) by an Cd-bearing Ag–Sb–Cu sulfosalt (b); sample 241, I #35747.

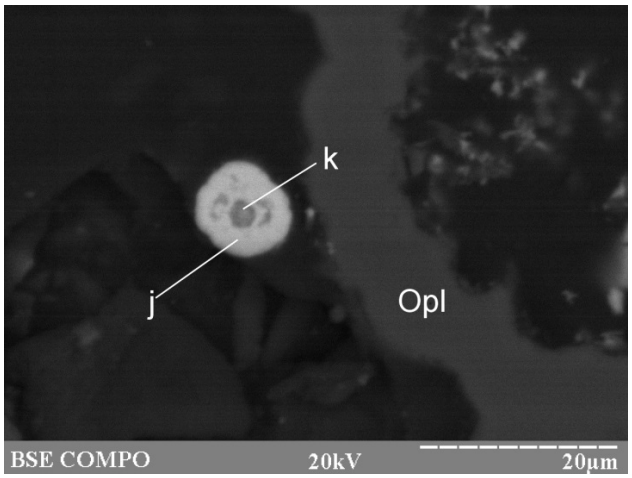

Figure S1-23. Zoned spherule with Ag-Sb-bearing covellite in the center (k) replaced by an Ag–Sb–Cu sulfosalt (j); sample 241, I #35739.

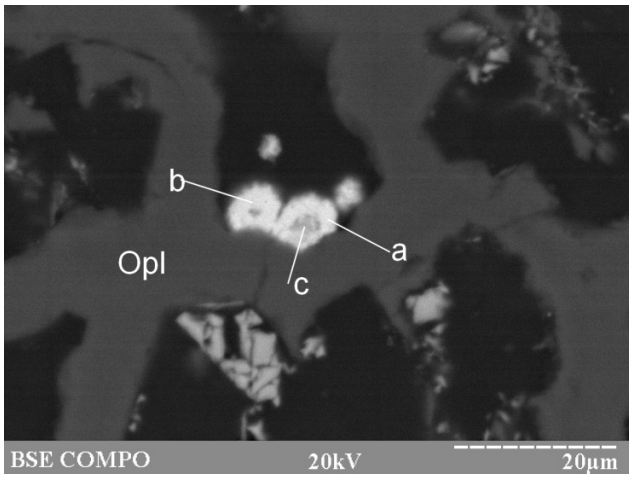

Figure S1-24. Reniform aggregates exhibiting the replacement of Ag-Sb-bearing covellite (c) by an Ag–Cu–Sb sulfosalt (a, b); sample 241, I #35736.

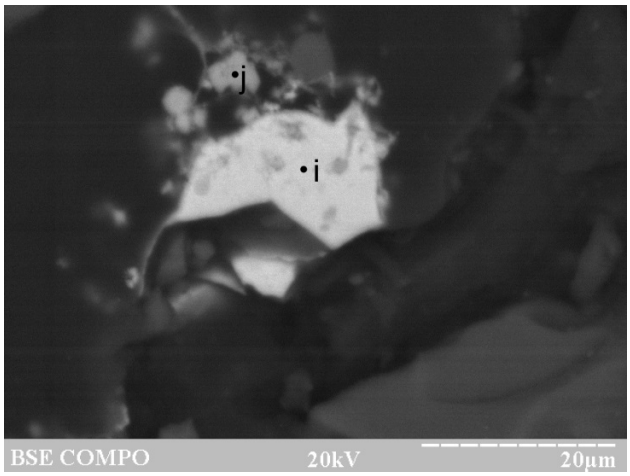

Figure S1-25. Assemblage of Ag-Sb-bearing covellite (j) and a Cu-bearing Ag–Sb sulfosalt ("pyrargyrite") (i); sample 241, I #35719.

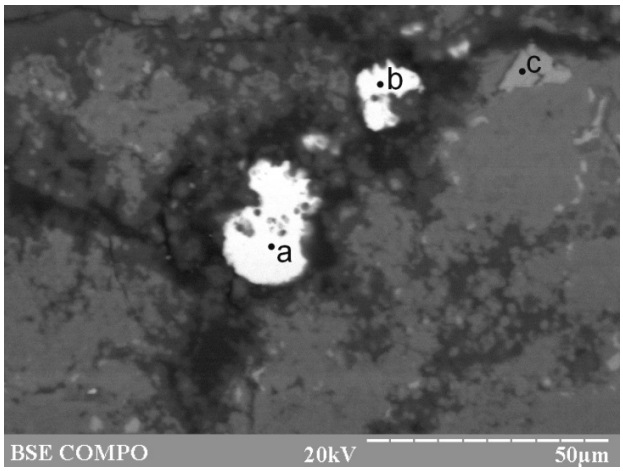

Figure S1-26. Galena (a, b) and relict high-Fe Zn sulfide (c) in Fe-oxyhydroxides; sample 241-2/2-5, I #34899.

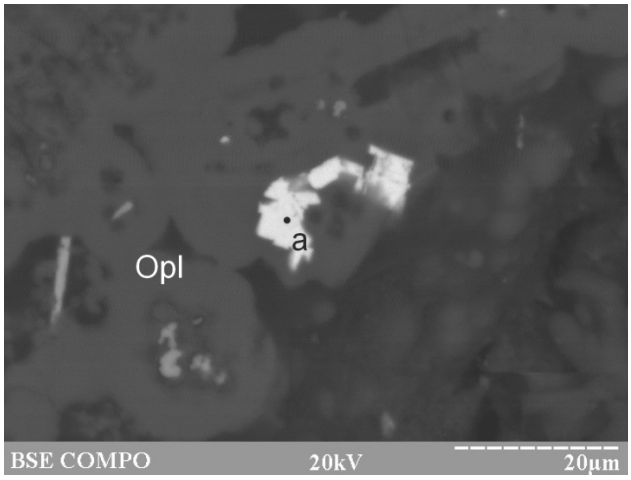

Figure S1-27. Interstitial galena crystals (a) in opal; sample 241-2/2-2, I #35659.

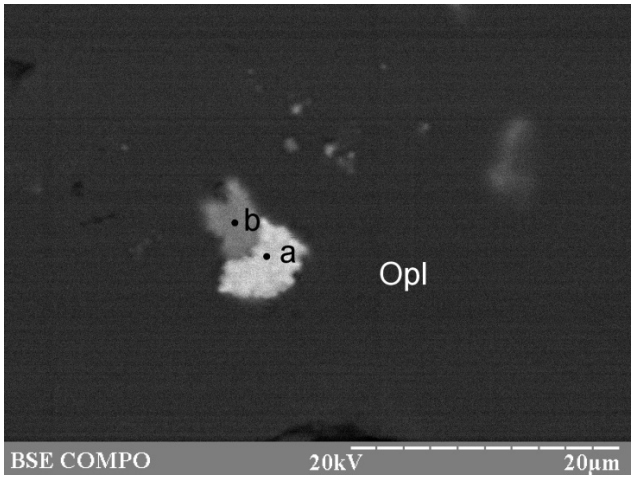

Figure S1-28. Replacement of sphalerite (b) by As-bearing galena (a) in opal; sample 241, I #35753.

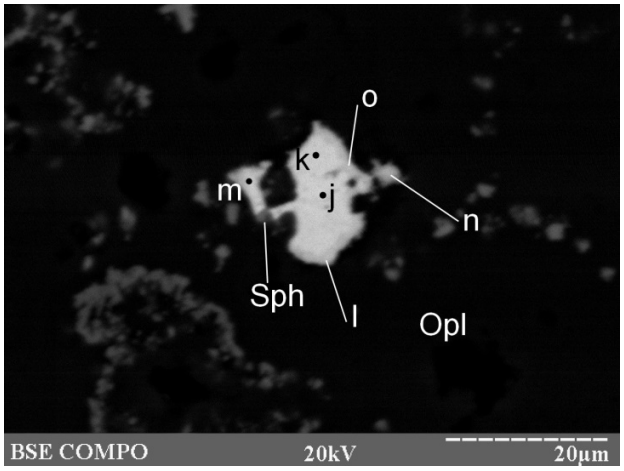

Figure S1-29. As-bearing galena crystals (j) replaced by a secondary As–O phase (other points); sample 241, I #35745.

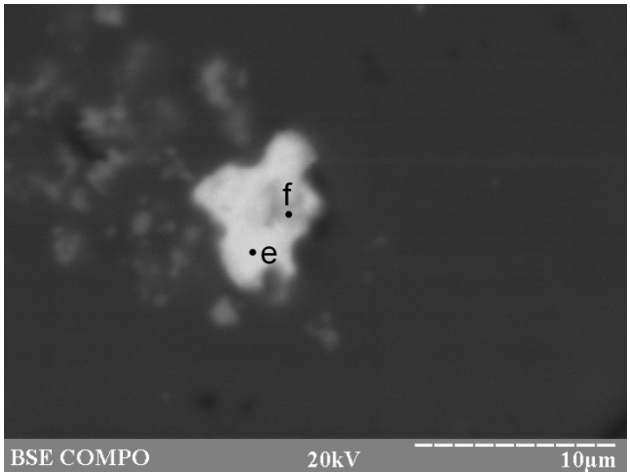

Figure S1-30. As-bearing galena crystals (e) replaced by a secondary As–O phase (f); sample 241, I #35743.

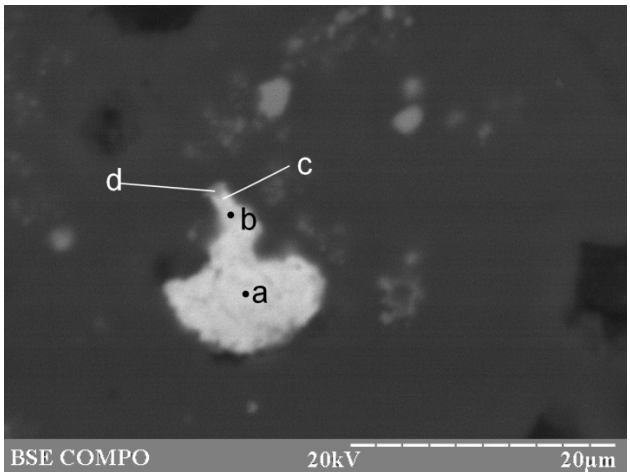

Figure S1-31. As-free (a) and As-bearing galena grains (b, c) replaced by a a secondary As–O phase (d); sample 241, I #35742.

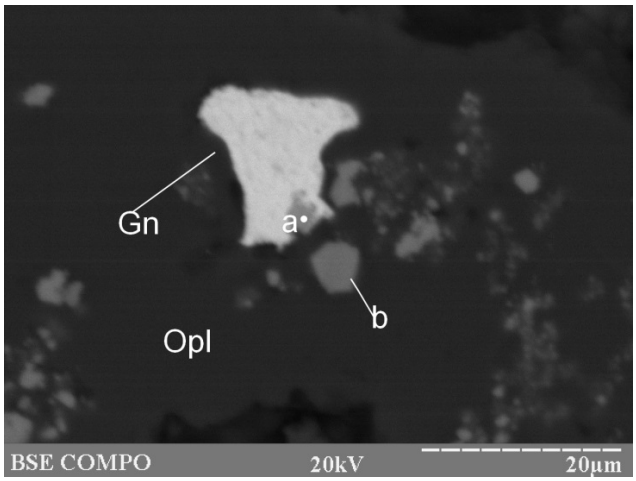

Figure S1-32. Replacement of galena by Ag- and Cd-bearing Zn sulfide (a) and inclusions of high-Fe Cd-free Zn sulfide in opal (b); sample 241, I #35717.

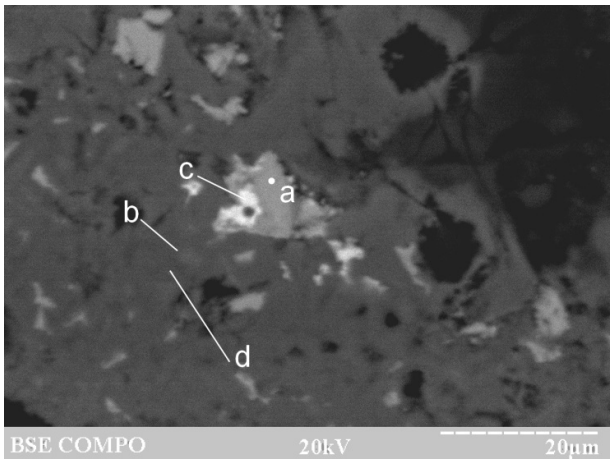

Figure S1-33. High-Fe sphalerite (a) with inclusions of an Au–Cu–S phase (c) replaced by Fe-oxyhydroxides (b, d); sample 241-2/2-4, I #35757.

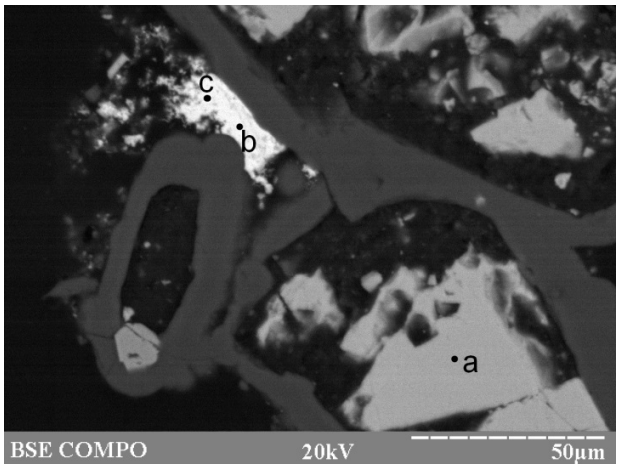

Figure S1-34. High-Fe Zn sulfide crystals (a) overgrown by opal with an interstitial Ag–Sb–Cu sulfosalt (c, b); sample 241-2/1-11, I #34921.

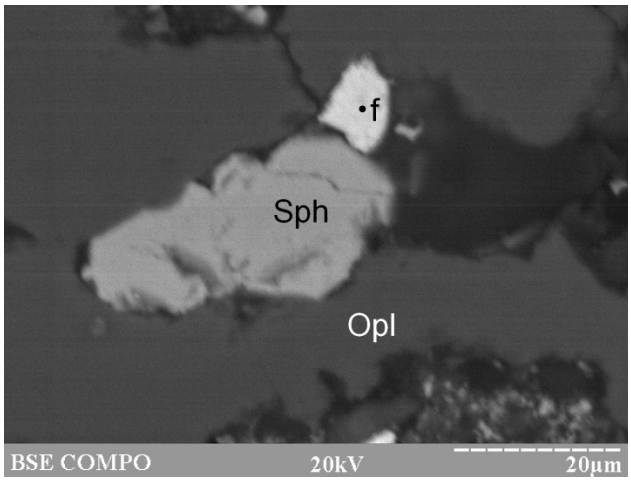

Figure S1-35. Aggregate of sphalerite and As-bearing Cu-bearing Ag–Sb sulfosalt ("miargyrite"); sample 241, I #35750.

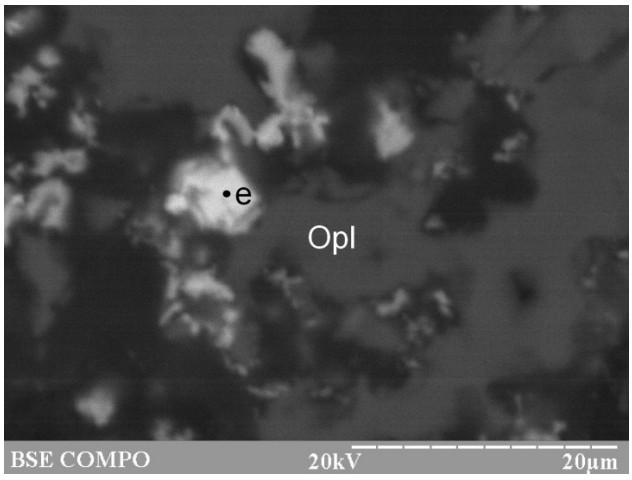

Figure S1-36. Interstitial aggregates of an Ag–Sb–Cu sulfosalt (e); sample 241, I #35749.

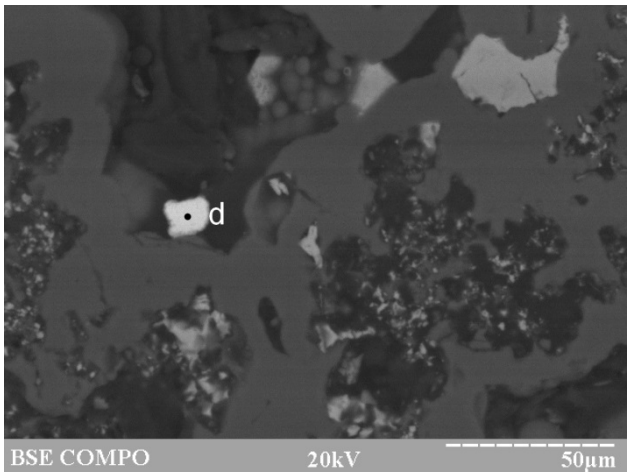

Figure S1-37. Subhedral crystal of Cu-bearing Ag–Sb sulfosalt ("argentotetrahedrite-Zn") (d) on opal; sample 241, I #35748.]

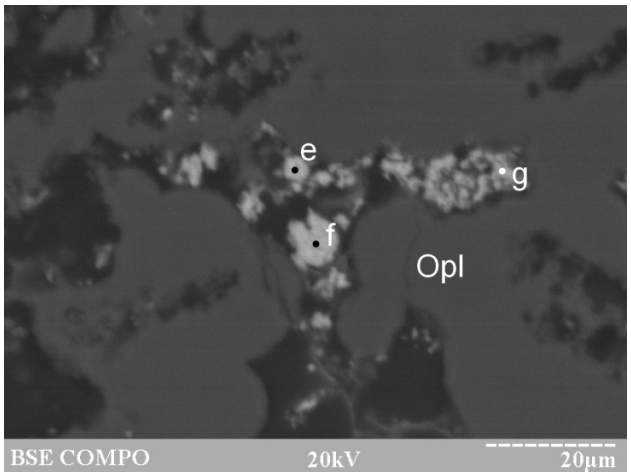

Figure S1-38. Interstitial aggregates of Ag-rich covellite (f), (g) and yarrowite (e) in opal; sample 241, I #35706.

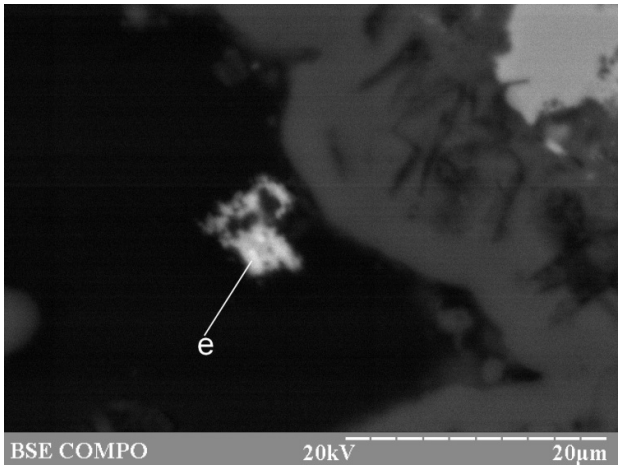

Figure S1-39. Cu–Ag–Sb sulfosalt (e) on opal with acicular native sulfur inclusions; sample 241-2/2-2, I #35655.

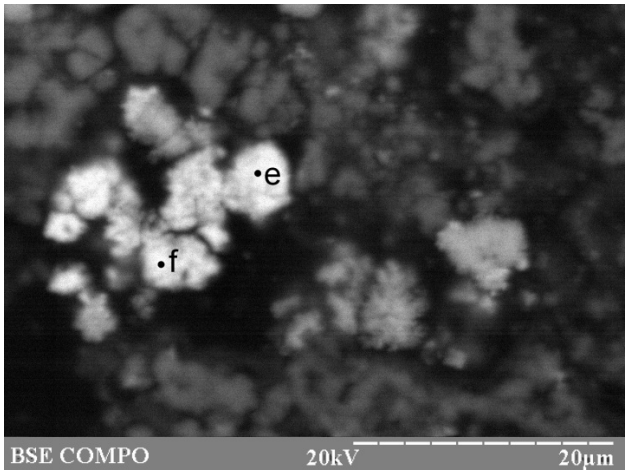

Figure S1-40. Granular aggregates of Cu-bearing acanthite (e, f); sample 241-2/2-5, I #34897.

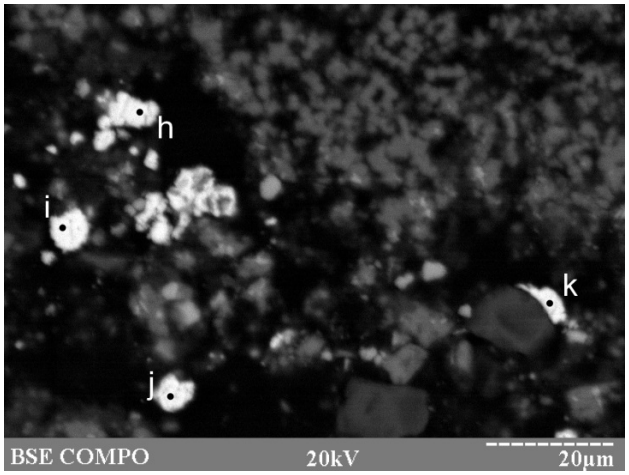

Figure S1-41. Fe-bearing acanthite grains (all points); sample 241-2/2-5, I #34901.

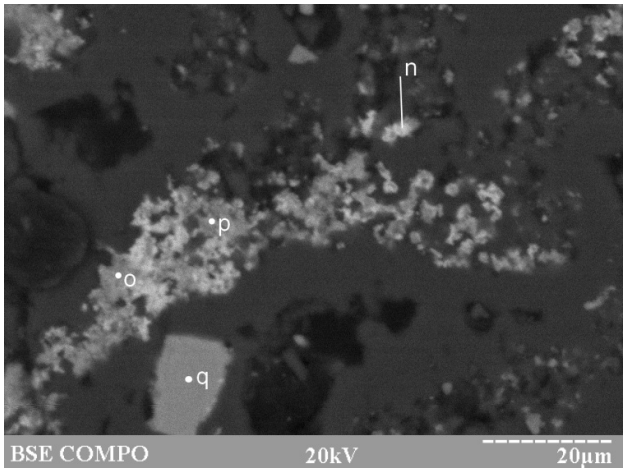

Figure S1-42. Sphalerite (q) replaced by fine aggregates of acanthite (n, p) locally intergrown with Cu sulfide (o); sample 241-2/1-11, I #34986.

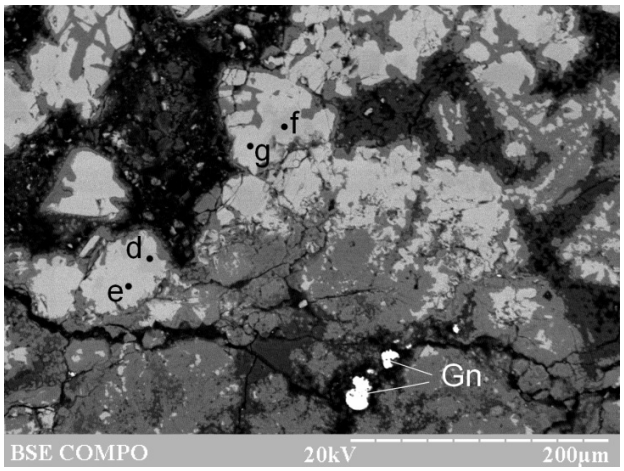

Figure S1-43. Wurtzite (e, g) and isocubanite (d, f) aggregates replaced by Fe-oxyhydroxides (dark gray); sample 241-2/2-5, I #34900.

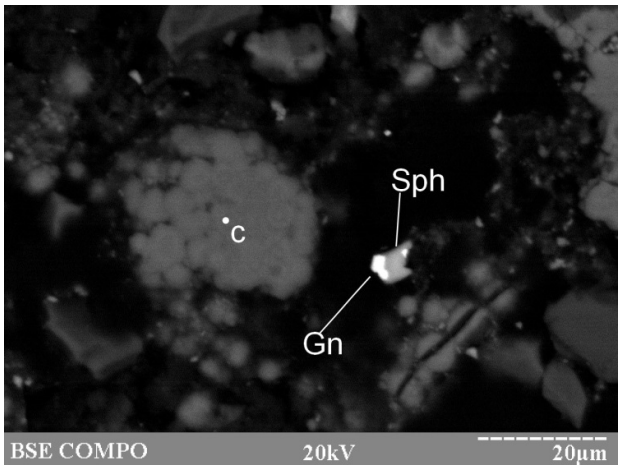

Figure S1-44. Fe-oxyhydroxides after spherulitic opal (c) and galena–sphalerite aggregate; sample 241-2/2-5, I #34992.

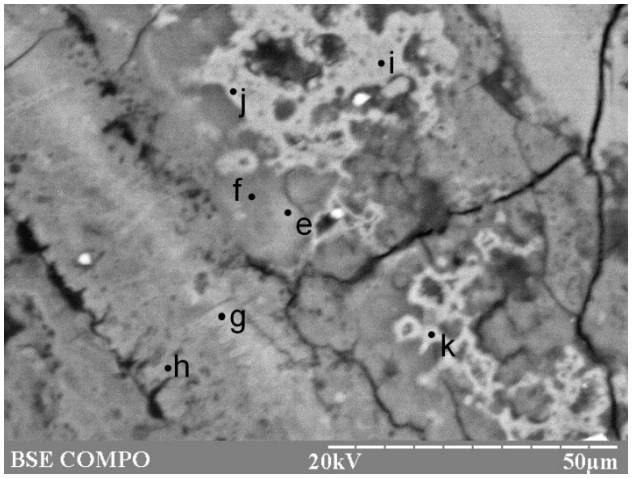

Figure S1-45. P-bearing Fe-oxyhydroxides of the outermost crust of Zn-rich chimney (i, j, k) replaced by P-bearing Mn-oxyhydroxides (h, g, f, e); sample 241-2/2-5, I #36258.

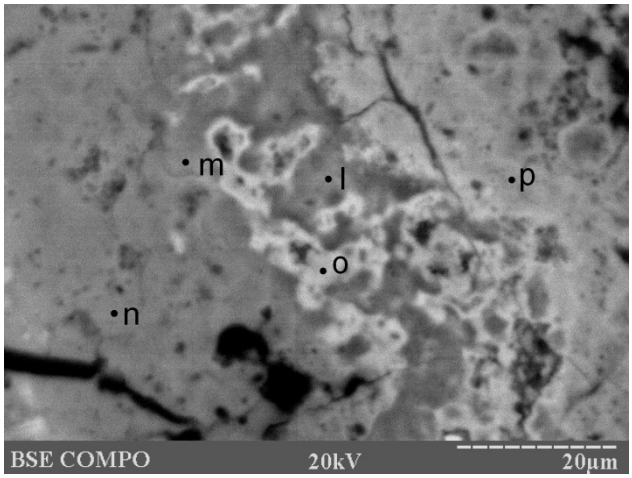

Figure S1-46. P-bearing Fe-oxyhydroxides of the outermost crust of Zn-rich chimney (o, p) replaced by P-bearing Mn-oxyhydroxides (l, m, n); sample 241-2/2-5, I #36259.

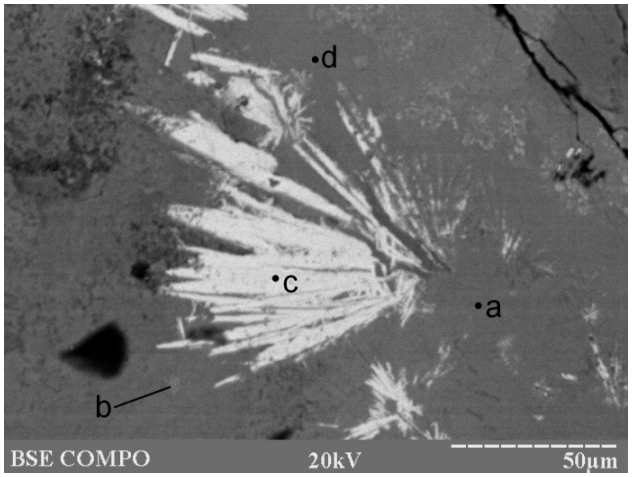

Figure S1-47. Radial barite aggregate (c) replaced by Fe-oxyhydroxides (a, b, d), sample 241-2/2-5, I #36457.

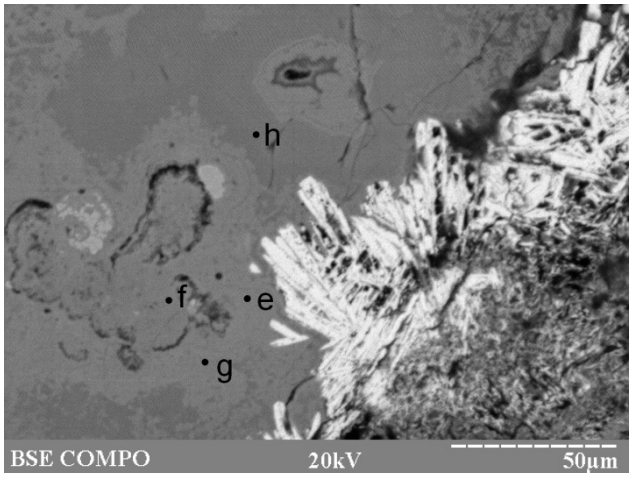

Figure S1-50. Radial barite aggregate (white) replaced by Fe-oxyhydroxides (e–h), sample 241-2/2-5, I #36458.

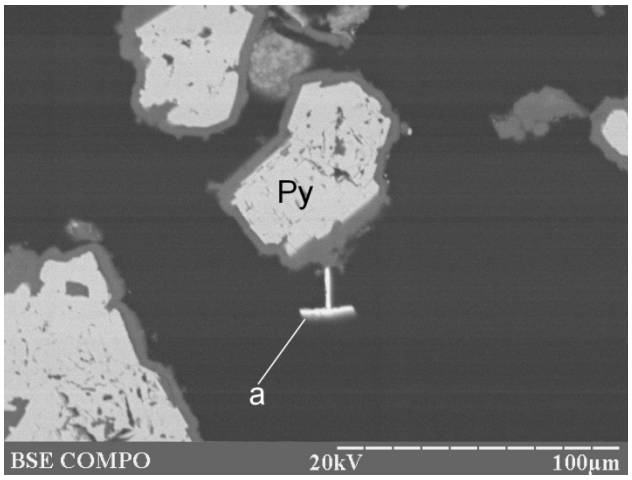

Figure S1-49. Barite crystals (a) on top of pyrite crystal rimmed by opal; sample 241-2/2-2, I #35627.

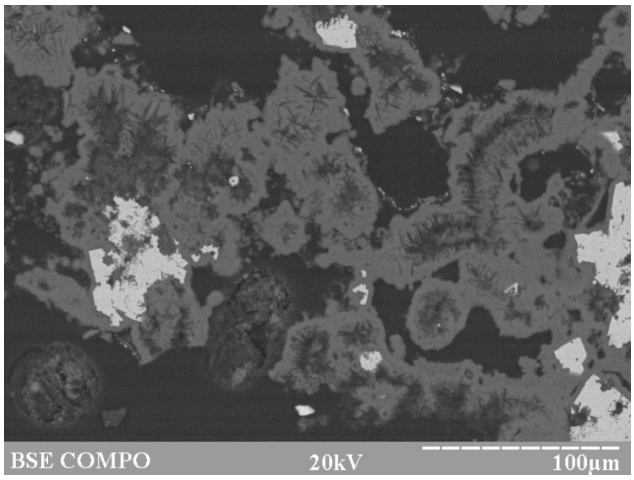

Figure S1-50. Radial aggregates of acicular native sulfur crystals rimmed by opal; sample 241-2/2-2, I #35623.

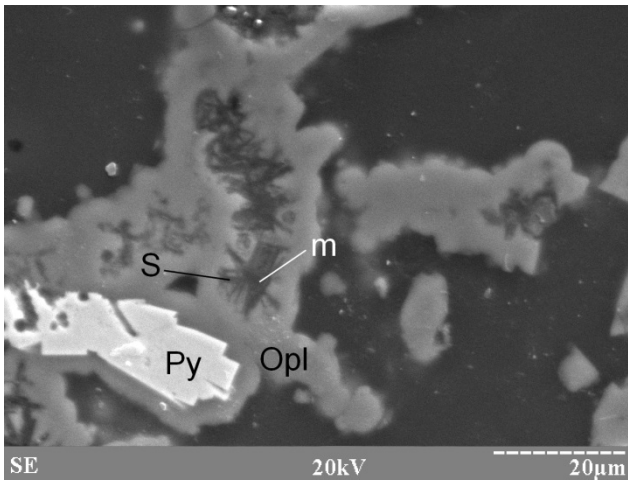

Figure S1-51. Radial aggregates of acicular native sulfur crystals rimmed by opal; sample 241-2/2-2, I #35622.

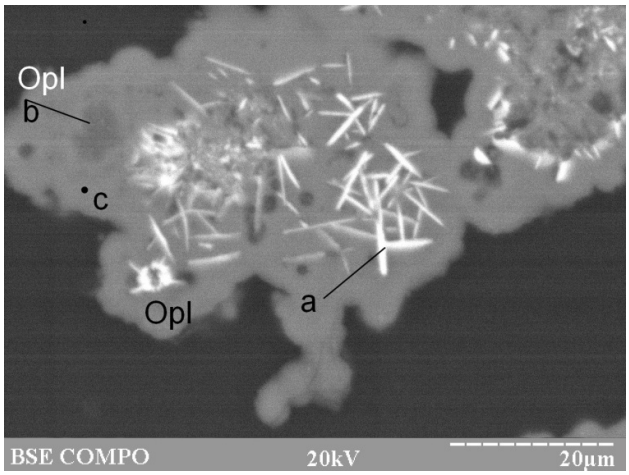

Figure S1-52. Acicular pyrrhotite crystals (a) overgrown by Al-rich opal (b) and low-Al opal (c); sample 241-2/2-2, I #35653.